

The two-channel Kondo effect in coupled interacting helical liquids

Sourav Biswas,^{1,*} Alessandro De Martino,^{2,†} Sumathi Rao,^{3,‡} and Arijit Kundu^{1,§}

¹*Department of Physics, Indian Institute of Technology - Kanpur, Kanpur 208 016, India.*

²*Department of Mathematics, City, University of London, EC1V 0HB London, UK*

³*International Centre for Theoretical Sciences (ICTS-TIFR),
Shivakote, Hesarahatta Hobli, Bangalore 560089, India*

(Dated: April 11, 2023)

We study the two-channel Kondo effect in the context of two interacting helical liquids coupled to a spin- $\frac{1}{2}$ magnetic impurity. We show that interactions between the two helical liquids significantly affect the phase diagram and other observable properties. Using a multichannel Luttinger liquid formalism, we analyze both the Toulouse limit, where an exact solution is available, and the weak coupling limit, which can be studied via a perturbative renormalization group (RG) approach. We recover the results for the ‘decoupled’ limit (interactions between the helical liquids switched off) and point out deviations from the known results due to this coupling. The perturbative RG study shows that each of the channels can flow to either a Ferromagnetic (FM) or an Anti-Ferromagnetic (AFM) fixed point. We obtain the phase diagram of the coupled system as a function of the system parameters. Observable consequences of the coupling are captured using linear response theory, which shows the scaling of the temperature as a function of the inter-channel interaction parameters.

I. INTRODUCTION

Topological systems have been at the center of research in condensed matter physics due to their exotic properties, one of them being topologically protected boundary modes [1–3]. In two dimensions such boundary modes become one-dimensional channels. One can find an energy window where the low-energy physics of the system is primarily described by the edge modes. Time reversal symmetry (TRS) plays a crucial role in many of these systems. In the case of Quantum Spin Hall insulators, the existence of the boundary modes depends on the TRS of the bulk. These systems host helical channels at the edge of the sample [4–6].

A peculiarity of one dimension is that, in spite of the presence of Coulomb interaction, the system remains exactly solvable, under certain conditions. It is well understood that the interacting physics of these edge modes is described by the Luttinger liquid (LL) theory [7–9]. The applicability of the LL formalism can be attributed to the linear dispersion of the edge states at low energies and to the topological protection against various back-scattering processes. However, such systems are not exactly solvable in the presence of impurities. Here, we are interested to study the effect of a single magnetic impurity on the one-dimensional channels formed at the boundary of two-dimensional topological systems, taking Coulomb interaction into account. The LL formed by the helical channel in presence of Coulomb interaction is termed helical liquid (HL).

It is well known that the Kondo effect describes the interaction between conduction electrons and a localized magnetic moment [10–15]. This phenomenon can also be investigated when Coulomb interaction is present in the conduction channel [16, 17]. So far, there have been studies addressing the problem of a spin- $\frac{1}{2}$ magnetic impurity coupled to a single helical liquid [18–21], as well as to two helical liquids [22–25]. In particular, Posske et al. [22] have studied the problem of two helical liquids decoupled from each other and coupled to a magnetic impurity. They have considered the Toulouse limit, where the model is exactly solvable, and have analyzed the decay of the Kondo cloud as function of temperature.

Here, we study a model of two interacting helical liquids coupled to a spin- $\frac{1}{2}$ magnetic impurity, allowing for forward scattering processes between the two helical liquids which preserve the symmetries of the bare Hamiltonian. We show that the inclusion of all forward scattering processes allowed by symmetry modifies the properties of the system and has observable consequences. The model can be mapped to a model of two decoupled channels interacting with the impurity. For a specific set of parameters values (the so-called Toulouse point) the mapping is essentially an Emery-Kivelson [26] mapping, which reduces the interacting system to an exactly solvable two-channel resonant-level model [26–28]. Away from the Toulouse point, the mapping still works, but the model is no longer solvable. We then use perturbative renormalization group techniques to study the effects of the Kondo interaction. Perturbative RG techniques have been very instrumental in the study of Kondo effects [7, 10, 11]. One can use this technique to study the fixed points of the model, even though the model is not exactly solved. One can further look into how these fixed points are modified as a function of system parameters. We note that previously the effect of scalar disorder has been studied in the context of two Luttinger liquids set-

* souravbw@iitk.ac.in

† Alessandro.De-Martino.1@city.ac.uk

‡ sumathi.rao@icts.res.in

§ arijit.hri@gmail.com

up [29, 30] using multichannel Luttinger liquid (MLL) formalism. Our analysis extends the study of impurity in multichannel Luttinger liquid set-up to magnetic impurities as well.

The plan for the rest of the paper is as follows. In Sec. II, we introduce the model of two interacting helical liquids coupled to a spin- $\frac{1}{2}$ impurity. We diagonalize the interaction terms (without the impurity) and, by using unitary transformations, recast the coupling to the Kondo impurity into a simpler form. In Sec. III, we focus on the Toulouse point, where the model can be reduced to an exactly solvable one, and compute the impurity spectral function. In Sec. IV, we move away from the exactly solvable point and use the perturbative renormalization group (RG) method to obtain the Kondo temperatures for both channels and to study the fixed points as function of the system parameters. In Sec. V, we present the explicit form of the conductance as a function of the temperature. Finally, in Sec. VI, we present our conclusions and provide an outlook. Throughout this paper we set $\hbar = 1$.

II. MODEL

We consider a system of two interacting helical liquids coupled to a magnetic impurity expressed by the model Hamiltonian $H = H_{\text{LL}} + H_{\text{K}}$, where H_{LL} describes the bulk of the HLs and H_{K} represents a magnetic impurity coupled to the HLs. The bulk Hamiltonian takes the well-known form $H_{\text{LL}} = H_0 + H_{\text{int}}$, where H_0 is the bare part and H_{int} accounts for the Coulomb interaction present in the HLs. We begin by writing the bare part of the model as [4, 5, 7–9]

$$H_0 = -i \sum_{j,s} s v_j \int dx \Psi_{j,s}^\dagger \partial_x \Psi_{j,s}, \quad (1)$$

where $\Psi_{j,s}$ are the field operators for the j^{th} channel, with $j \in \{1, 2\}$, and v_j are the Fermi velocities. We assume that the right-moving modes, denoted by $s = +$, carry spin up and the left-moving modes, denoted by $s = -$, carry spin down.

Next, we write down the interacting part of the model arising from the Coulomb interaction. We allow forward scattering processes between the two channels, which we write as

$$H_{\text{int}} = \int dx \left[g_4^{(1)} (\rho_{1R}^2 + \rho_{1L}^2) + 2g_2^{(1)} \rho_{1R} \rho_{1L} + g_4^{(2)} (\rho_{2R}^2 + \rho_{2L}^2) + 2g_2^{(2)} \rho_{2R} \rho_{2L} + 2g_4^{(12)} (\rho_{1R} \rho_{2R} + \rho_{1L} \rho_{2L}) + 2g_2^{(12)} (\rho_{1R} \rho_{2L} + \rho_{1L} \rho_{2R}) \right], \quad (2)$$

where $\rho_{j,s} = \Psi_{j,s}^\dagger \Psi_{j,s}$ is the fermionic density operator. Here g_2^{ζ}, g_4^{ζ} follow the standard g -ology convention with g_2^{ζ} denoting forward scattering processes involving density operators of movers in opposite directions and g_4^{ζ} denoting processes with movers in the same direction. The

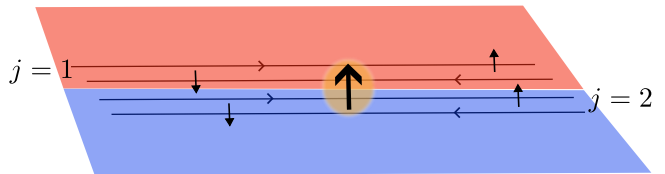


FIG. 1. Schematic picture of the system under study. Two helical liquids, labelled by the index $j = 1, 2$, propagate along the translational invariant direction \hat{x} . The right-moving fermions carry an up-spin (\uparrow) index and the left-moving fermions a down-spin (\downarrow) index. The two helical liquids are in close proximity to each other and are coupled to a spin- $\frac{1}{2}$ impurity, located at $x = 0$.

superscript $\zeta = 1, 2$ denotes scattering within individual channels $j = 1, 2$, whereas $\zeta = 12$ denotes scattering involving both channels. We note that the bare Hamiltonian H_0 is topologically protected and the terms included in Eq. (2) are allowed by symmetry. In addition, these interacting liquids are coupled to a spin- $\frac{1}{2}$ impurity, with the Kondo Hamiltonian given by

$$H_{\text{K}} = \sum_{j,s} J_{z,j} s \Psi_{j,s}^\dagger(0) \Psi_{j,s}(0) \sigma^z + \sum_{j=1,2} J_{\perp,j} \left(\Psi_{j,+}^\dagger(0) \Psi_{j,-}(0) \sigma^- + \text{h.c.} \right), \quad (3)$$

where $J_{z,j}$ and $J_{\perp,j}$ are the Kondo couplings for the j^{th} channel, and $\sigma^{\pm} = \sigma^x \pm i\sigma^y$ are the spin- $\frac{1}{2}$ operators for the impurity located at $x = 0$.

To proceed further, we employ the bosonization technique [31–33]. Since a HL has the same number of degrees of freedom as a spinless LL [18], two bosonic fields ϕ_j, θ_j are sufficient to bosonize the Hamiltonian H . We bosonize the fermion operator using the identity [31–33]

$$\Psi_{j,s} = (2\pi\xi_j)^{-1/2} e^{-i\sqrt{\pi}(\theta_j - s\phi_j)}, \quad (4)$$

where ξ_j is a microscopic cut-off length corresponding to channel j . The Klein factors have been neglected since they always appear in pairs in the quantities of interest we compute. We note that $\rho_{j,s} = \frac{1}{2\sqrt{\pi}} \partial_x (\phi_j - s\theta_j)$ and $\Pi_j = \partial_x \theta_j$. By combining the bosonized forms of H_0 and H_{int} , we arrive at the multichannel Luttinger liquid (MLL) Hamiltonian

$$H_{\text{LL}} = H_0 + H_{\text{int}} = \frac{1}{2} \int dx \left(\partial_x \Phi^T M_\phi \partial_x \Phi + \partial_x \Theta^T M_\theta \partial_x \Theta \right), \quad (5)$$

where we have used the notation $\Phi = (\phi_1 \ \phi_2)^T$, $\Theta = (\theta_1 \ \theta_2)^T$ and

$$M_\phi^{ij} = \left(v_i + \frac{g_4^{(i)} + g_2^{(i)}}{\pi} \right) \delta_{ij} + \frac{g_4^{(12)} + g_2^{(12)}}{\pi} (1 - \delta_{ij}), \quad (6)$$

$$M_\theta^{ij} = \left(v_i + \frac{g_4^{(i)} - g_2^{(i)}}{\pi} \right) \delta_{ij} + \frac{g_4^{(12)} - g_2^{(12)}}{\pi} (1 - \delta_{ij}). \quad (7)$$

We can now diagonalize H_{LL} using standard methods (see, e.g., [34, 35]). We assume that H_{LL} is diagonal in $\tilde{\Theta}$ and $\tilde{\Phi}$ fields, where $\tilde{\Phi} = (\tilde{\phi}_1 \ \tilde{\phi}_2)^T$, $\tilde{\Theta} = (\tilde{\theta}_1 \ \tilde{\theta}_2)^T$ and $\tilde{\Pi}_j = \partial_x \tilde{\theta}_j$. These fields are related to the Φ and Θ fields via linear transformations $\Phi = V_\phi \tilde{\Phi}$ and $\Theta = V_\theta \tilde{\Theta}$ such that $\tilde{\Theta}^T \tilde{\Phi} = \Theta^T \Phi$. The explicit forms of V_ϕ and V_θ are found as

$$V_\phi = U_\phi^T D_\phi^{-\frac{1}{2}} \mathcal{U}^T \mathcal{D}^{\frac{1}{4}}, \quad (8)$$

$$V_\theta = U_\theta^T D_\theta^{\frac{1}{2}} \mathcal{U}^T \mathcal{D}^{-\frac{1}{4}}, \quad (9)$$

where U_ϕ is a matrix that diagonalizes M_ϕ of Eq. (5), D_ϕ is a diagonal matrix with eigenvalues of M_ϕ as its diagonal entries. The orthogonal matrix \mathcal{U} and the diagonal matrix \mathcal{D} are obtained from the product of matrices $D_\phi^{\frac{1}{2}} U_\phi M_\theta U_\phi^T D_\phi^{\frac{1}{2}}$ by diagonalizing as $D_\phi^{\frac{1}{2}} U_\phi M_\theta U_\phi^T D_\phi^{\frac{1}{2}} = \mathcal{U}^T \mathcal{D} \mathcal{U}$. This procedure enables us to write the two-channel Luttinger liquid Hamiltonian $H_{\text{LL}} = H_0 + H_{\text{int}}$ as

$$H_{\text{LL}} = \sum_{j=1,2} \frac{u_j}{2} \int dx \left[(\partial_x \tilde{\theta}_j)^2 + (\partial_x \tilde{\phi}_j)^2 \right], \quad (10)$$

where the renormalized velocities u_j are the diagonal entries of $\mathcal{D}^{\frac{1}{2}}$. The Kondo Hamiltonian can be written in terms of the new fields as

$$H_{\text{K}} = \sum_{j=1,2} \left[-\frac{\tilde{J}_{z,j}}{\sqrt{\pi}} \tilde{\Pi}_j(0) \sigma^z + \frac{J_{\perp,j}}{2\pi\xi_j} \left(e^{i2\sqrt{\pi}[V_\phi^{j1}\tilde{\phi}_1(0)+V_\phi^{j2}\tilde{\phi}_2(0)]} \sigma^+ + \text{h.c.} \right) \right], \quad (11)$$

where

$$\tilde{J}_{z,j} = \sum_{k=1,2} J_{z,k} V_\theta^{kj}. \quad (12)$$

At this point, we make a short digression to understand the decoupled limit from the calculations done so far. We notice that if we neglect the inter-channel interactions, $g_{2,4}^{(12)} = 0$, then $M_{\phi,\theta}$ are diagonal. Hence V_ϕ and V_θ are also diagonal and given by $V_\phi^{ij} = \sqrt{K_j} \delta_{ij}$ and $V_\theta^{ij} = \delta_{ij} / \sqrt{K_j}$, where

$$K_j = \sqrt{1 + \frac{g_4^{(j)} - g_2^{(j)}}{\pi v_j}} / \sqrt{1 + \frac{g_4^{(j)} + g_2^{(j)}}{\pi v_j}}$$

is the usual Luttinger liquid parameter for channel j . Therefore, $\tilde{\phi}_j = \phi_j / \sqrt{K_j}$, $\tilde{\Pi}_j = \sqrt{K_j} \Pi_j$, $u_j = v_j / K_j$, and $\tilde{J}_{z,j} = J_{z,j} / \sqrt{K_j}$, and we recover the Hamiltonian considered in [22, 24].

The Hamiltonian (10) describes two effectively decoupled HLs obtained by the diagonalization procedure when $g_{2,4}^{(12)} \neq 0$. The new decoupled fields $\tilde{\phi}_j$ have been used to rewrite the Kondo Hamiltonian. We observe from

Eq. (11) that both fields $\tilde{\phi}_1$ and $\tilde{\phi}_2$ appear in each of the exponential terms of H_{K} . This is a manifestation of the finite inter-channel scattering processes $g_{2,4}^{(12)}$. Hence, even if H_{LL} can be cast into a diagonal form, the Kondo term still couples the two fields. We proceed further to reduce the full Hamiltonian H to a Hamiltonian describing two decoupled interacting channels coupled to a single Kondo impurity, by devising a unitary transformation $U_{\text{d}} = e^{i2\sqrt{\pi}(\lambda_1 \tilde{\phi}_1(0) + \lambda_2 \tilde{\phi}_2(0)) \sigma^z}$ and choosing $\lambda_{1,2}$ appropriately to arrive at $\tilde{H} \equiv U_{\text{d}} H U_{\text{d}}^\dagger$ given by

$$\tilde{H} = \sum_{j=1,2} \left[\frac{u_j}{2} \int dx \left[\tilde{\Pi}_j^2 + (\partial_x \tilde{\phi}_j)^2 \right] - \frac{\tilde{J}'_{z,j}}{\sqrt{\pi}} \tilde{\Pi}_j(0) \sigma^z + \frac{J_{\perp,j}}{2\pi\xi_j} \left(e^{i2\sqrt{\pi}\kappa_j \tilde{\phi}_j(0)} \sigma^+ + \text{h.c.} \right) \right], \quad (13)$$

where

$$\kappa_j = V_\phi^{jj} - V_\phi^{\bar{j}j} \quad \text{and} \quad \tilde{J}'_{z,j} = \tilde{J}_{z,j} - 2\pi u_j V_\phi^{\bar{j}j}. \quad (14)$$

Here, $\bar{j} = 2, 1$ for $j = 1, 2$. We refer to App. A for the details of the derivation. We use this Hamiltonian in Sec. IV to derive the RG flow of the Kondo couplings.

Alternatively, we can use the unitary transformation to cancel the $\tilde{J}_{z,j}$ -terms. This is accomplished by setting $\lambda_j = -\frac{\tilde{J}_{z,j}}{2\pi u_j}$, as shown in App. A. We then arrive at

$$\tilde{H} = \sum_{j=1,2} \left[\frac{u_j}{2} \int dx \left[\tilde{\Pi}_j^2 + (\partial_x \tilde{\phi}_j)^2 \right] + \frac{J_{\perp,j}}{2\pi\xi_j} \left(e^{i2\sqrt{\pi} \sum_k \kappa_{jk} \tilde{\phi}_k(0)} \sigma^+ + \text{h.c.} \right) \right], \quad (15)$$

where we have defined

$$\kappa_{jk} = V_\phi^{jk} - \frac{\tilde{J}_{z,k}}{2\pi u_k}. \quad (16)$$

This Hamiltonian is the starting point for the calculation of observables. In the next section, we study a particular limit in which H is exactly solvable and in Sec. IV we use the perturbative RG approach to study the weak coupling limit beyond the solvable point.

Before moving on, we briefly comment on the nonlinear interaction terms that have been omitted in the interacting Hamiltonian H . In general, the inclusion of interaction-induced backscattering operators can open a gap and render the gapless Luttinger liquid physics invalid. However, an helical liquid is topologically protected against intra-channel backscattering terms. We consider here a regime in which also the inter-channel backscattering terms are negligible [9]. Furthermore, we assume that the system is away from half-filling and neglect all Umklapp processes [9], as further discussed App. B. Finally, we have taken into account only the intra-channel Kondo spin-flip scatterings as the source of possible backscattering in the system and have dropped the inter-channel Kondo couplings.

III. EXACTLY SOLVABLE POINT

In this section, we show that for special values of the system parameters the model admits an exact solution [26, 38]. In fact, for the Hamiltonian (15), there are two possible sets of conditions under which the mapping can be achieved. The first set of conditions is

$$\kappa_{11} = \kappa_{22} = 0, \quad \kappa_{12}^2 = \kappa_{21}^2 = \frac{1}{2}. \quad (17)$$

The first condition ensures that the two channels decouple, i.e., only one field appears in each exponential operator in the Kondo interaction. The second ensures that the Kondo interaction has the scaling dimension of a fermionic field. Using Eq. (16), this set of conditions can be written in terms of V_ϕ and $\tilde{J}_{z,j}$ as

$$\tilde{J}_{z,1} = 2\pi u_1 V_\phi^{11}, \quad \tilde{J}_{z,2} = 2\pi u_2 V_\phi^{22}, \quad (18)$$

$$(V_\phi^{11} - V_\phi^{21})^2 = (V_\phi^{22} - V_\phi^{12})^2 = \frac{1}{2}. \quad (19)$$

These conditions can only be satisfied when V_ϕ is a non-diagonal matrix. When these conditions hold, the two-channel Kondo problem can be explicitly mapped to a resonant-level problem [26–28]. Since V_ϕ is a function of the system parameters, we need the solution in terms of the values of the system parameters.

Note that the alternative choice

$$\kappa_{12} = \kappa_{21} = 0, \quad \kappa_{11}^2 = \kappa_{22}^2 = \frac{1}{2} \quad (20)$$

becomes

$$\tilde{J}_{z,1} = 2\pi u_1 V_\phi^{21}, \quad \tilde{J}_{z,2} = 2\pi u_2 V_\phi^{12}, \quad (21)$$

$$(V_\phi^{11} - V_\phi^{21})^2 = (V_\phi^{22} - V_\phi^{12})^2 = \frac{1}{2}. \quad (22)$$

We see that Eq. (22) is precisely the same as Eq. (19). Both choices lead to the reduction of Eq. (15) to a resonant-level model with two non-interacting channels coupled to a single magnetic impurity. Since the exact solution depends on relationships between different parameters of the model, it is clear that as the parameter values change, it is only for certain values that we will get an exact solution. In Fig. 2 we plot the two conditions $(V_\phi^{11} - V_\phi^{21})^2 - \frac{1}{2} \equiv V_{sol}^1 = 0$ and $(V_\phi^{22} - V_\phi^{12})^2 - \frac{1}{2} \equiv V_{sol}^2 = 0$ as a function of two parameters at a time (the other parameters have been fixed at the values given in Table I). Then, the intersections of the curves $V_{sol}^1 = 0$ and $V_{sol}^2 = 0$ give the points where an exact solution is possible. As discussed in the previous section, one has to choose the parameters in a way such that Eq. (15) is sufficient to describe all possible scattering processes. Following the analysis done in App. B, we make the choice of the parameters in a way such that

$$\frac{1}{4} \sum_{j=1,2} (V_\theta^{1j} - V_\theta^{2j})^2 + \frac{1}{4} \sum_{j=1,2} (V_\phi^{1j} \mp V_\phi^{2j})^2 > 1. \quad (23)$$

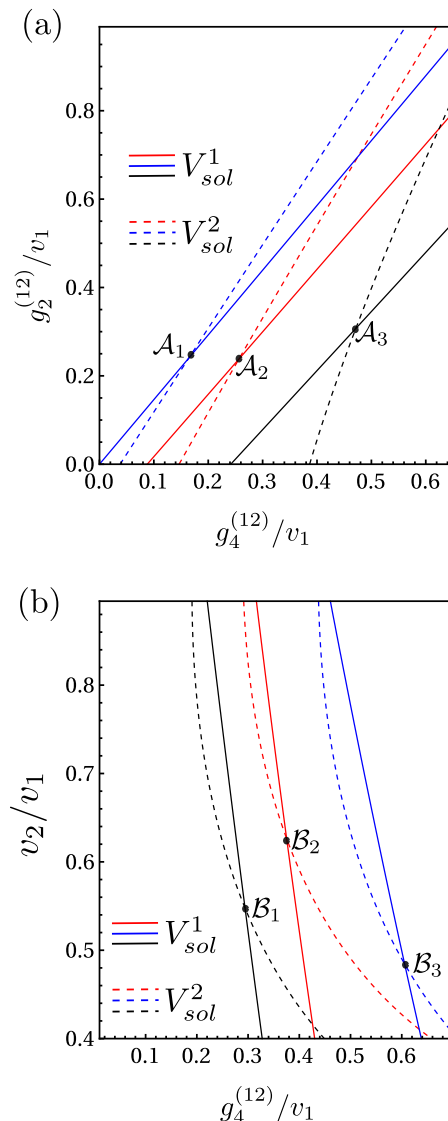


FIG. 2. Two lines given by $V_{sol}^1 = 0$ and $V_{sol}^2 = 0$ are plotted as a function of system parameters. The intersection of these two lines denotes an exactly solvable point, where the model can be transformed into a model of two non-interacting channels coupled to a single impurity. These intersections are denoted by separate symbols \mathcal{A}_j and \mathcal{B}_j . Changing the system parameters shifts the exact solution. In (a) we have varied $g_2^{(12)}$ and $g_4^{(12)}$. The origin corresponds to decoupled limit of the problem and we can clearly see a shift from that limit. In (b), v_2 and $g_4^{(12)}$ are varied. All the parameters are scaled by v_1 . The other parameters which are required to generate this plot are listed in Table I.

The choice of the parameters for the mapping to the resonant level model has been made in a way such that the vertex operator, $e^{i2\sqrt{\pi} \sum_k \kappa_{jk} \hat{\phi}_k(0)}$ can be refermionized using the same bosonization identity that we used earlier so that the model reduces to that of free fermions. We can write the non-chiral boson fields used for describ-

	v_2/v_1	$g_2^{(1)}/v_1$	$g_2^{(2)}/v_1$	$g_4^{(1)}/v_1$	$g_4^{(2)}/v_1$	$g_2^{(12)}/v_1$	$g_4^{(12)}/v_1$
\mathcal{A}_1	1.5	2.0π	2.4π	2.2π	2.5π
\mathcal{A}_2	0.5	1.25π	1.4π	1.4π	1.5π
\mathcal{A}_3	0.4	1.2π	1.4π	1.6π	1.5π
\mathcal{B}_1	...	1.45π	1.475π	1.6π	1.6π	0.35	...
\mathcal{B}_2	...	1.45π	1.475π	1.5π	1.5π	0.5	...
\mathcal{B}_3	...	1.45π	1.65π	1.6π	1.75π	0.75	...

TABLE I. Values of the system parameters used in Fig. 2. The blank boxes with dots stand for the parameters which are varied in the plots.

ing the HL as $\tilde{\phi}_j = (\tilde{\phi}_{j,L} + \tilde{\phi}_{j,R})$ and $\tilde{\theta}_j = (\tilde{\phi}_{j,L} - \tilde{\phi}_{j,R})$ where R and L denote the right and left movers. In order to cast the Hamiltonian as an exactly solvable non-interacting fermion model, we first focus on the Luttinger liquid defined on the positive and negative x -axis, separately. The system on the right and left half-lines is “unfolded” [26, 31, 39] so that the Hamiltonian is presented in a chiral form. We follow the convention that on the positive x -axis $\tilde{\phi}_{j,R}(x) = \tilde{\phi}_{j,R}^e(x)$ and $\tilde{\phi}_{j,L}(x) = \tilde{\phi}_{j,R}^e(-x)$. One can obtain two chiral liquids in the bulk of the channel using these identities. Then, one must identify the chiral boson fields to be equal at $x = 0$ i.e. $\tilde{\phi}_{j,L}^e(0) = \tilde{\phi}_{j,R}^e(0)$. We notice that the Kondo scattering term is defined only at $x = 0$. One has to choose one chiral field out of $\tilde{\phi}_{j,R}^e(0)$ and $\tilde{\phi}_{j,L}^e(0)$, to write the vertex operator of the Kondo interaction term. After doing so the Hamiltonian can again be written on the full line in terms of chiral fields only. However, depending on the choice of the chiral field used to write down the vertex operator in the Kondo scattering term, one chiral field remains decoupled from the impurity and can be discarded from the resonant level model as it has an independent free solution. In what follows, we use the right-moving bosonic field to write down the exact solution. The bosonization identity $\Psi_j = (2\pi\xi_j)^{-1/2} e^{i2\sqrt{\pi}\tilde{\phi}_{j,R}^e}$ can be used to write the model in terms of fermions. In this limit Eq. (15) can be expressed in terms of chiral spinless fermions $\Psi_j(x)$ [19] as

$$H_T = \sum_j \left[-iu_j \int dx \Psi_j^\dagger(x) \partial_x \Psi_j(x) + \epsilon_d d^\dagger d + \frac{J_{\perp,j}}{\sqrt{2\pi\xi_j}} \left(d^\dagger \Psi_j(0) + \Psi_j^\dagger(0) d \right) \right], \quad (24)$$

where the impurity spin residing at $x = 0$ has been modeled by a discrete level, such that $\sigma_z = d^\dagger d - 1/2$. The operator d^\dagger creates a spinless fermion in the discrete level and ϵ_d is the chemical potential at the site of the discrete level. We refer to App. C for the details of the exact solution. At the exactly solvable point, one can self-consistently compute the energy spectrum and the impurity spectral function [40]. In our case, the spectral function turns out to be a Lorentzian with a level width

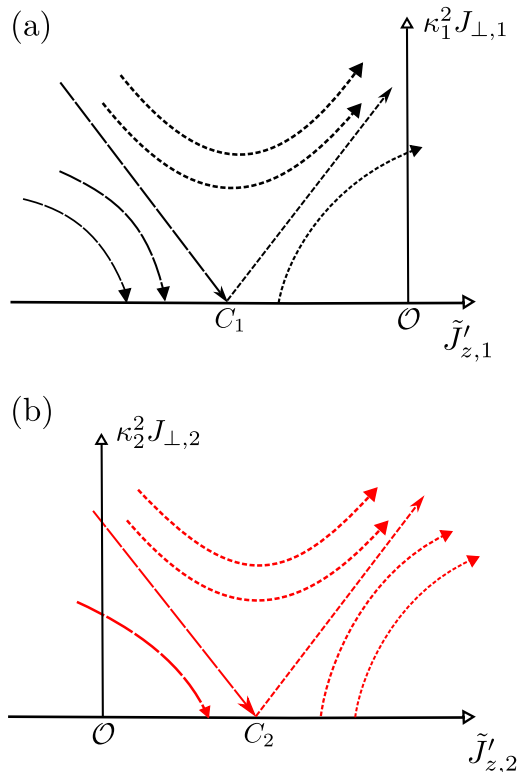


FIG. 3. Schematic representation of the RG flow in Eqs. (27) and (28). In panel (a) and (b) we show two sets of flow trajectories pertaining to the two different channels. The symbol \mathcal{O} denotes the point $(J_{\perp,j}, \tilde{J}'_{z,j}) = (0, 0)$. The position of the starting point of the trajectory relative to C_j (rather than to \mathcal{O}) determines whether the system flows to a FM or an AFM fixed point.

$\Gamma = \sum_j \frac{J_{\perp,j}^2}{4\pi\xi_j u_j}$. We see that the two contributions coming from the two independent channels add up directly.

In the decoupled limit (which can be obtained by switching off the interchannel forward scattering processes $g_{2,4}^{(12)}$), our result matches with one of the exactly solvable points derived in [22]. In this limit, $M_{\phi,\theta}$ are diagonal and $K_j = \kappa_j^2 = (V_\phi^{jj})^2$. We have chosen $\kappa_j = 1/\sqrt{2}$ and as a result $K_1 + K_2 = 1$. We note that our exact solution does not require the channels to have equal velocities. In fact, due to the presence of off-diagonal terms in $M_{\phi,\theta}$, the normalized velocities of the diagonalized Hamiltonian are not equal in our case. At the exactly solvable point choosing $K_j = 1$ leads to an effectively non-interacting fermionic model coupled to magnetic impurity, if inter-channel processes are switched off. This particular limit is not of our interest. However we note, this would lead to another exactly solvable limit derived in [22].

IV. BEYOND THE EXACTLY SOLVABLE LIMIT

In this section, we use the perturbative renormalization group technique to analyze the flow of the Kondo couplings [41, 42]. By using the effectively decoupled Hamiltonian in Eq. (13), we find that for each channel j the RG equations (up to second order in the couplings) are given by

$$\frac{d\tilde{J}'_{z,j}}{dl} = \nu_j \kappa_j^3 J_{\perp,j}^2, \quad (25)$$

$$\frac{dJ_{\perp,j}}{dl} = (1 - \kappa_j^2) J_{\perp,j} + \nu_j \kappa_j \tilde{J}'_{z,j} J_{\perp,j}, \quad (26)$$

where $\nu_j \equiv \frac{1}{\pi u_j}$ [?]. We emphasize that the MLL formalism is instrumental in mapping the results to a form similar to the known one-channel counterpart [7, 18, 41]. The details of the derivation are provided in the App. D. The equations (25) and (26) can be put in a more compact form by defining $\nu_j \bar{J}_{z,j} = \nu_j \kappa_j \tilde{J}'_{z,j} + 1 - \kappa_j^2$ as

$$\frac{d\bar{J}_{z,j}}{dl} = \nu_j \kappa_j^4 J_{\perp,j}^2, \quad (27)$$

$$\frac{dJ_{\perp,j}}{dl} = \nu_j \bar{J}_{z,j} J_{\perp,j}. \quad (28)$$

The trajectories of the flow equations are given by $(\kappa_j^2 J_{\perp,j})^2 - (\bar{J}_{z,j})^2 = c$, where c is a constant. It is known that a single channel either flows to an anti-ferromagnetic (AFM) or a ferromagnetic (FM) fixed point (FP) [10, 18]. Earlier works have shown how the RG flow in such a system depends on the Luttinger parameter [7, 18]. In our case, each of the effectively decoupled channels behaves like a single Luttinger liquid wire and can flow to either FM- or AFM-FP separately. However, the inclusion of inter-channel interactions in Eq. (2) modifies the range of parameters of the system for which the couplings flow either to the FM or the AFM fixed point.

We plot a schematic flow diagram pertaining to the above RG equations in Fig. 3. If the Kondo couplings of channel j of Eq. (13) flow to infinity then the impurity is strongly coupled with channel j . On the other hand, if $J_{\perp,j}$ renormalizes to zero then the impurity is weakly coupled with channel j . The transition point C_j separates the $\tilde{J}'_{z,j}$ axis into two portions having opposite flows. To study different FPs, we choose $J_{\perp,j} = 0$ of Fig. 3 as the initial condition. On this line whether the system flows to FM or AFM fixed point is decided by the position of C_j .

In Fig. 3, the position of the transition point C_j on $\tilde{J}'_{z,j}$ axis depends on the solution of $\nu_j \kappa_j \tilde{J}'_{z,j} + 1 - \kappa_j^2 = 0$. We known from Eq. (14) that $\kappa_j = V_{\phi}^{jj} - V_{\phi}^{\bar{j}j}$. Hence, we see that inter-channel interactions shift the position of the transition point on $\tilde{J}'_{z,j}$ axis. As long as $\kappa_j \neq 1$ the transition point does not lie at $\tilde{J}'_{z,j} = 0$ which we denote by \mathcal{O} .

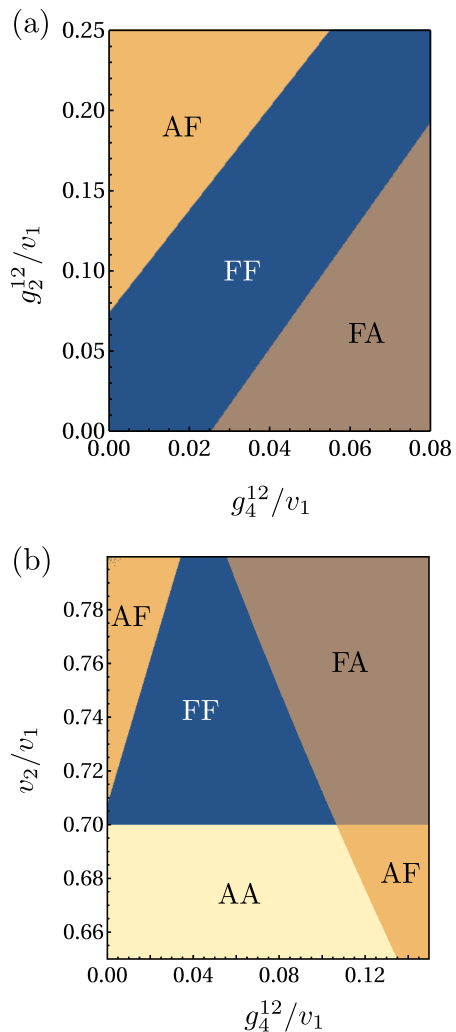


FIG. 4. The above diagrams show the different FPs to which the two channels flow, as a function of the system parameters. We refer to these diagrams of the parameter space as phase diagrams. Each of the effectively decoupled channels can flow to either the A or the F fixed point, starting from $J_{\perp,j} = 0$, (see the discussion in the main text). In panel (a) we set $v_2/v_1 = 0.75$, $g_2^{(1)}/v_1 = 0.65\pi$, $g_2^{(2)}/v_1 = 0.7\pi$, $g_4^{(1)}/v_1 = 1.275\pi$, $g_4^{(2)}/v_1 = 1.5\pi$. In panel (b) we set $g_2^{(1)}/v_1 = 0.5\pi$, $g_2^{(2)}/v_1 = 0.6\pi$, $g_4^{(1)}/v_1 = 1.2\pi$, $g_4^{(2)}/v_1 = 1.4\pi$, $g_2^{(12)}/v_1 = 0.175$.

Next, we look into the RG flow of each of the effectively decoupled channels of Eq. (13). It is easy to identify, from Fig. 3(b), that for $\kappa_2 > \kappa_2^{-1}$ there is a region on the positive $\tilde{J}'_{z,2}$ axis between C_2 and \mathcal{O} , where even if the Kondo coupling is positive i.e. AFM like, the system flows to an FM fixed point. We denote these fixed points by F. By the same token, a channel can flow to an AFM FP despite being expected to flow to an FM FP. Such FPs are denoted by A. For example in Fig. 3(a), the transition point C_1 lies to the left of \mathcal{O} and FPs of type A are obtained for the choice $\kappa_1 < \kappa_1^{-1}$. We can combine these FPs of both the channels and name them ' $\mathcal{P}_j \mathcal{P}_{j'}$ ',

where \mathcal{P}_j denotes the FP of channel j and can be either A or F. Once we have identified the fixed points we can study their dependence on different parameters, as shown in Fig. 4. These parameters have to be chosen in a way such that conditions written down in Eq. (23) are satisfied. We note that similar analysis can also be done for different choices of $J_{\perp,j}$, as an initial condition.

From Eqs. (25) and (26), we can calculate the Kondo temperature for the two channels. We define $\alpha^j = \sqrt{(\tilde{J}'_{z,j,0})^2 / (J_{\perp,j,0})^2 - 1}$, where $\tilde{J}'_{z,j,0}$, $J_{\perp,j,0}$ are the bare values of the $\tilde{J}'_{z,j}$, $J_{\perp,j}$ couplings. With Λ being the bandwidth of the original system, the Kondo temperature T_K^j for channel j is given by

$$T_K^j = \Lambda \exp\left(-\frac{\sinh^{-1}(\alpha_j)}{\alpha_j \nu_j J_{\perp,j,0}}\right). \quad (29)$$

We note that T_K^j is the characteristic energy scale of the Kondo effect pertaining to each of these channels.

V. OBSERVABLE CONSEQUENCE

The presence of a magnetic impurity modifies the conductance of the HLs by contributing a correction, $\delta\mathcal{G}(\omega)$, originating from spin-flip scattering processes mediated by the Kondo effect. This correction vanishes for HLs as temperature $T \rightarrow 0$ and also in the DC limit when frequency $\omega \rightarrow 0$ [18–21]. However, the signature of Kondo scattering can still be captured by computing the correction at non-zero T and ω . In order to study the scaling of the correction to the conductance, we compute $\delta\mathcal{G}(\omega)$ in response to an external potential \mathcal{V} , in the weak coupling regime. This implies $\delta\mathcal{G}(\omega) \ll e^2$, e being the electron charge.

Following [19], we add $H_{1,\mathcal{V}} = -\frac{e\mathcal{V}}{2} \int dx \tilde{\Pi}_1$ and $H_{2,\mathcal{V}} = -\frac{e\mathcal{V}}{2} \int dx \tilde{\Pi}_2$ to the Hamiltonian defined in Eq. (15). The total contribution coming from these two terms is the same as that obtained by attaching $H_{\mathcal{V}} = -e\mathcal{V}\sigma^z$ to the Hamiltonian of Eq. (15). Hence $[\tilde{H}, H_{\mathcal{V}} - (H_{1,\mathcal{V}} + H_{2,\mathcal{V}})] = 0$ and we can compute transport properties in response to spin-flip current using $H_{\mathcal{V}}$. One can use the Kubo formula [21, 40] to compute this correction. The details of the calculation are given in App. E. One can write down the exact expressions for the conductance correction in the limit $J_{\perp,j}^2 \ll \omega \ll T$. The correction to conductance due to Kondo scattering scales as

$$\delta\mathcal{G}(\omega) = \mathcal{L}_1 T^{2(\kappa_{11}^2 + \kappa_{12}^2) - 2} + \mathcal{L}_2 T^{2(\kappa_{21}^2 + \kappa_{22}^2) - 2} + \mathcal{L}_3 T^{2(\kappa_{11}\kappa_{12} + \kappa_{22}\kappa_{21}) - 2}, \quad (30)$$

where

$$\mathcal{L}_1 = -\frac{e^2}{4} \left(\frac{J_{\perp,1}}{2\pi\xi_1}\right)^2 \left(\frac{2\pi}{\Lambda}\right)^{2\kappa_{11}^2} \left(\frac{2\pi}{\Lambda}\right)^{2\kappa_{12}^2} \left(\frac{1}{\pi}\right)^2 \frac{\pi\Gamma(\kappa_{11}^2 + \kappa_{12}^2)^2}{\Gamma(2(\kappa_{11}^2 + \kappa_{12}^2))}, \quad (31)$$

$$\mathcal{L}_2 = -\frac{e^2}{4} \left(\frac{J_{\perp,2}}{2\pi\xi_2}\right)^2 \left(\frac{2\pi}{\Lambda}\right)^{2\kappa_{21}^2} \left(\frac{2\pi}{\Lambda}\right)^{2\kappa_{22}^2} \left(\frac{1}{\pi}\right)^2 \frac{\pi\Gamma(\kappa_{21}^2 + \kappa_{22}^2)^2}{\Gamma(2(\kappa_{21}^2 + \kappa_{22}^2))}, \quad (32)$$

$$\mathcal{L}_3 = -\frac{e^2}{2} \frac{J_{\perp,1}J_{\perp,2}}{(2\pi)^2\xi_1\xi_2} \left(\frac{2\pi}{\Lambda}\right)^{2(\kappa_{11}\kappa_{12})} \left(\frac{2\pi}{\Lambda}\right)^{2\kappa_{22}\kappa_{21}} \left(\frac{1}{\pi}\right)^2 \frac{\pi\Gamma(\kappa_{11}\kappa_{12} + \kappa_{22}\kappa_{21})^2}{\Gamma(2(\kappa_{11}\kappa_{12} + \kappa_{22}\kappa_{21}))}. \quad (33)$$

At the exactly solvable limit \mathcal{L}_3 is ill-defined. However, this term drops out from the expression of conductance before we go to the limit $J_{\perp,j}^2 \ll \omega \ll T$, as discussed in App. E.

VI. DISCUSSION

In this work we have presented a general framework for studying two interacting helical liquids coupled to a Kondo impurity, including both intra-channel as well as inter-channel interactions.

We have derived the conditions under which an exact solution of the model can be obtained with the additional restriction of $\kappa_j = 1/\sqrt{2}$, where κ_j is defined in

Eq. (14). This solvable point has been calculated using an Emery-Kivelson type of transformation. We have extended the parameter space of the problem by including inter-channel forward scattering processes yielding exact solutions to the problem studied beyond the scenarios captured by Refs. [22, 26, 38]. In Sec. III we have shown how the exact solutions of the decoupled limit (obtained by switching off $g_{2,4}^{12}$) can be derived from our calculation. At the solvable point, we have calculated the spectral function. We have shown that the level width is the sum of contributions coming from each channel. The spectral function has experimental significance in the context of the physics of quantum dots as, the differential conductance is proportional to the spectral function [43–46].

Away from the exactly solvable point, the model can be

mapped to a pair of effectively decoupled HLs interacting with a single magnetic impurity, as derived in Eq. (13). By using a perturbative RG approach, we have shown that these two renormalized channels can separately flow to either the FM or the AFM fixed point. We note that here AFM fixed point indicates Kondo cloud formation, whereas the FM fixed point means the absence of the same, although a finite residual coupling can be present in the case of FM. In Fig. 3 we show a schematic flow diagram pertaining to the RG equations derived in Sec. IV. Fig. 4 shows the phase diagrams obtained from our RG analysis. As discussed in Sec. IV, two effectively decoupled HLs flow to these FPs as a result of renormalization. We have further shown the linear response of the system in the weak limit, which captures the trans-

port signature for two interacting HLs in presence of a magnetic impurity.

VII. ACKNOWLEDGMENTS

S.B. and A.K. acknowledges support from the DST (Govt. of India) via sanction no. DST/NM/TUE/QM-6/2019 (C)-IIT Kanpur. A.K. acknowledges support from the SERB (Govt. of India) via sanction no. ECR/2018/001443 and CRG/2020/001803, DAE (Govt. of India) via sanction no. 58/20/15/2019-BRNS, as well as MHRD (Govt. of India) via sanction no. SPARC/2018-2019/P538/SL.

Appendix A: Unitary transformations

Under the action of the unitary transformation

$$U = e^{i2\sqrt{\pi}(\lambda_1\tilde{\phi}_1(0)+\lambda_2\tilde{\phi}_2(0))\sigma^z}, \quad (\text{A1})$$

the Luttinger liquid Hamiltonian H_{LL} transforms as

$$H_{LL} \rightarrow \tilde{H}_{LL} = UH_{LL}U^\dagger = \sum_{j=1,2} \left[\frac{u_j}{2} \int dx \left[\tilde{\Pi}_j^2 + (\partial_x \tilde{\phi}_j)^2 \right] - 2\sqrt{\pi}\lambda_j u_j \tilde{\Pi}_j(0)\sigma^z \right], \quad (\text{A2})$$

while the Kondo Hamiltonian H_K transforms as

$$H_K \rightarrow \tilde{H}_K = UH_KU^\dagger = \sum_{j=1,2} \left[-\frac{\tilde{J}_{z,j}}{\sqrt{\pi}} \tilde{\Pi}_j(0)\sigma^z + \frac{J_{\perp,j}}{2\pi\xi_j} \left(e^{i2\sqrt{\pi}[(V_\phi^{j1}+\lambda_1)\tilde{\phi}_1(0)+(V_\phi^{j2}+\lambda_2)\tilde{\phi}_2(0)]}\sigma^+ + \text{h.c.} \right) \right]. \quad (\text{A3})$$

(We have omitted an unimportant constant.) We then arrive at a decoupled-channel Hamiltonian with either of the two following equivalent choices:

$$\lambda_j = -V_\phi^{jj} \quad \text{or} \quad \lambda_j = -V_\phi^{\bar{j}j}. \quad (\text{A4})$$

(We use the notation $\bar{j} = 2, 1$ for $j = 1, 2$.) We select the second option, and collecting \tilde{H}_{LL} and \tilde{H}_K , we arrive at the Hamiltonian

$$\tilde{H} = \sum_{j=1,2} \left[\frac{u_j}{2} \int dx \left[\tilde{\Pi}_j^2 + (\partial_x \tilde{\phi}_j)^2 \right] - \frac{\tilde{J}'_{z,j}}{\sqrt{\pi}} \tilde{\Pi}_j(0)\sigma^z + \frac{J_{\perp,j}}{2\pi\xi_j} \left(e^{i2\sqrt{\pi}\kappa_j\tilde{\phi}_j(0)}\sigma^+ + \text{h.c.} \right) \right], \quad (\text{A5})$$

where we have defined

$$\tilde{J}'_{z,j} = \tilde{J}_{z,j} - 2\pi u_j V_\phi^{\bar{j}j}, \quad \kappa_j = V_\phi^{jj} - V_\phi^{\bar{j}j}. \quad (\text{A6})$$

We use this Hamiltonian for the calculation of the RG flow of the Kondo couplings in Sec. IV and App. D.

Alternatively, in the unitary transformation (A1) we can set $\lambda_j = -\frac{\tilde{J}_{z,j}}{2\pi u_j}$ and we obtain

$$\tilde{H} = \sum_{j=1,2} \left[\frac{u_j}{2} \int dx \left[\tilde{\Pi}_j^2 + (\partial_x \tilde{\phi}_j)^2 \right] + \frac{J_{\perp,j}}{2\pi\xi_j} \left(e^{i2\sqrt{\pi}\sum_k \kappa_{jk}\tilde{\phi}_k(0)}\sigma^+ + \text{h.c.} \right) \right], \quad (\text{A7})$$

where we have defined

$$\kappa_{jk} = V_\phi^{jk} - \frac{\tilde{J}_{z,k}}{2\pi u_k}. \quad (\text{A8})$$

We employ this form of the Hamiltonian in the discussion of the solvable point in Sec. III and for the perturbative calculation of the correction to the conductance in Sec. V.

Appendix B: Interaction Hamiltonian

In this appendix we establish the conditions under which it is justified to retain only the interaction terms included in Eq. (2). Following [9], the interaction Hamiltonian for a two-channel HL in general comprises terms that lead to nonlinearities in the bosonized theory. These terms include the Umklapp scattering processes

$$\Psi_{j\uparrow}^\dagger(x)\Psi_{j\uparrow}^\dagger(x+a)\Psi_{j\downarrow}(x+a)\Psi_{j\downarrow}(x)e^{-i4k_F x} + \text{h.c.}, \quad j = 1, 2. \quad (\text{B1})$$

We omit these processes on account of the fact that we consider the generic incommensurate situation, i.e., $4k_F$ different from a reciprocal lattice vector.

Next, let us consider Kondo scatterings between different channels. They are described by the following operators:

$$\Psi_{1,\uparrow}^\dagger\Psi_{2,\uparrow} - \Psi_{1,\downarrow}^\dagger\Psi_{2,\downarrow} \sim e^{i\sqrt{\pi}((V_\theta^{11}-V_\theta^{21})\tilde{\theta}_1+(V_\theta^{12}-V_\theta^{22})\tilde{\theta}_2)} \sin(\sqrt{\pi}((V_\phi^{11}-V_\phi^{21})\tilde{\phi}_1+(V_\phi^{12}-V_\phi^{22})\tilde{\phi}_2)), \quad (\text{B2})$$

$$\Psi_{1,\uparrow}^\dagger\Psi_{2,\downarrow} \sim e^{i\sqrt{\pi}((V_\theta^{11}-V_\theta^{21})\tilde{\theta}_1+(V_\theta^{12}-V_\theta^{22})\tilde{\theta}_2)} e^{-i\sqrt{\pi}((V_\phi^{11}+V_\phi^{21})\tilde{\phi}_1+(V_\phi^{12}+V_\phi^{22})\tilde{\phi}_2)}. \quad (\text{B3})$$

Calculating their scaling dimensions, we find that these terms are irrelevant (and can thus be omitted) if the following two conditions hold:

$$\frac{1}{4} \sum_{j=1,2} \left(V_\theta^{1j} - V_\theta^{2j} \right)^2 + \frac{1}{4} \sum_{j=1,2} \left(V_\phi^{1j} \mp V_\phi^{2j} \right)^2 > 1. \quad (\text{B4})$$

Appendix C: Two-channel resonant-level model

In this section, we briefly discuss the solution of Eq. (24). We Fourier transform the Hamiltonian in this equation to cast it into a resonant-level model consisting of two non-interacting channels coupled to a discrete level modeled by d operators. The Hamiltonian becomes

$$H_\Gamma = \sum_{k,j} \epsilon_{k,J} c_{k,j}^\dagger c_{k,j} + \epsilon_d d^\dagger d + \sum_{k,J} t_j \left[c_{k,j}^\dagger d + c_{k,j} d^\dagger \right]. \quad (\text{C1})$$

Here, $t_j = \frac{J_{\perp,j}}{\sqrt{4\pi^2\xi_j}}$ and $\epsilon_{k,j} = u_j k$. We look for new fermionic operators $f_n^\dagger = \sum_{k,j} M_{n,k}^j c_{k,j}^\dagger + L_n d^\dagger$ such that $H_\Gamma = \sum_n E_n f_n^\dagger f_n + \text{const.}$ We then have $[H_\Gamma, f_n^\dagger] = E_n f_n^\dagger$, and from Eq. (C1)

$$\left[H_\Gamma, f_n^\dagger \right] = \sum_{k,j} \left[M_{n,k}^j \epsilon_{k,j} c_{k,j}^\dagger + t_j M_{n,k}^j d^\dagger + t_j L_n c_{k,j}^\dagger \right] + \epsilon_d L_n d^\dagger. \quad (\text{C2})$$

We have used $[ab, c] = a\{b, c\} - \{a, c\}b$. Hence,

$$\begin{aligned} E_n f_n^\dagger &= \sum_{k,j} \left[M_{n,k}^j \epsilon_{k,j} c_{k,j}^\dagger + t_j M_{n,k}^j d^\dagger + t_j L_n c_{k,j}^\dagger \right] + \epsilon_d L_n d^\dagger, \\ E_n \left[\sum_{k,j} M_{n,k}^j c_{k,j}^\dagger + L_n d^\dagger \right] &= \sum_{k,j} \left[M_{n,k}^j \epsilon_{k,j} c_{k,j}^\dagger + t_j L_n c_{k,j}^\dagger \right] + \left[\sum_{k,j} t_j M_{n,k}^j d^\dagger + \epsilon_d L_n d^\dagger \right]. \end{aligned} \quad (\text{C3})$$

If we introduce a resonant level to a two independent channel set-up, then,

$$\begin{aligned} E_n M_{n,k}^j &= M_{n,k}^j \epsilon_{k,j} + t_j L_n, \\ E_n L_n &= \sum_j t_j \sum_k M_{n,k}^j + \epsilon_d L_n. \end{aligned} \quad (\text{C4})$$

One would get,

$$E_n = \sum_j t_j^2 \sum_k \frac{1}{E_n - \epsilon_{k,j}} + \epsilon_d. \quad (\text{C5})$$

The above equation can be graphically solved, for finite system [40]. We use the following relation [40] to evaluate the sum over k ,

$$\sum_{n=-\infty}^{\infty} \frac{1}{E_n - \pi n} = \cot(E_n). \quad (\text{C6})$$

For $\epsilon_d = 0$,

$$E_n = \sum_j \frac{\pi t_j^2}{u_j} \cot\left(\frac{E_n \pi}{u_j}\right). \quad (\text{C7})$$

One can solve the above equation numerically to obtain the energy E_n . We can further derive spectral function from the impurity Green's function. We note that in path integral formalism,

$$\begin{aligned} Z &= \int \mathcal{D}[d, c_j] e^{-S} = \int \mathcal{D}[d] e^{-S_d} \int \mathcal{D}[c] e^{-S_c}, \\ S_d &= \int_0^\beta d\tau \left[\bar{d}(\partial_\tau + \epsilon_d) d \right], \\ S_c &= \sum_j \int_0^\beta d\tau \left[\sum_k \bar{c}_{k,j} (\partial_\tau + \epsilon_{k,j}) c_{k,j} + \sum_k (t_j \bar{c}_{k,j} d + c_{k,j} \bar{d}) \right]. \end{aligned} \quad (\text{C8})$$

From the above expressions we can write,

$$\begin{aligned} Z &= \int \mathcal{D}[d] e^{-\int_0^\beta d\tau \left[\bar{d}(\partial_\tau + \epsilon_d) d \right]} \int \mathcal{D}[c_1] e^{-\int_0^\beta d\tau \left[\sum_k \bar{c}_{k,1} (\partial_\tau + \epsilon_{k,1}) c_{k,1} + \sum_k (t_{\alpha} \bar{c}_{k,1} d + c_{k,1} \bar{d}) \right]} \\ &\quad \int \mathcal{D}[c_2] e^{-\int_0^\beta d\tau \left[\sum_k \bar{c}_{k,2} (\partial_\tau + \epsilon_{k,2}) c_{k,2} + \sum_k (t_{\alpha} \bar{c}_{k,2} d + c_{k,2} \bar{d}) \right]}. \end{aligned} \quad (\text{C9})$$

One can integrate out $c_{k,j}$'s to obtain,

$$Z \sim \int \mathcal{D}[d] \exp \left[- \int_0^\beta d\tau \bar{d} (\partial_\tau + \epsilon_d - \sum_j \frac{t_j^2}{\partial_\tau + \epsilon_{k,j}}) d \right]. \quad (\text{C10})$$

here we are showing the relevant term which depends on d operators. We next perform Fourier transformation $d(\tau) = \beta^{-1/2} \sum_n d_n e^{-i\omega_n \tau}$, where ω_n is n^{th} Matsubara frequency and β is inverse temperature. This enables us to replace ∂_τ by $-i\omega_n$.

$$Z \sim \int \mathcal{D}[d] \exp \left[- \sum_{i\omega_n} \bar{d}_n (-i\omega_n + \epsilon_d - \sum_j \frac{t_j^2}{i\omega_n + \epsilon_{k,j}}) d_n \right]. \quad (\text{C11})$$

Hence the impurity green's function can be written as

$$G_d(i\omega_n) = \frac{1}{i\omega_n - \epsilon_d + i\Gamma \text{sgn}(\omega_n)}. \quad (\text{C12})$$

and the spectral function, defined as $-\frac{1}{\pi} \text{Im}(G_d)$, becomes a Lorentzian with width,

$$\Gamma = \sum_j \Gamma_j = \sum_j \pi \frac{t_j^2}{u_j}. \quad (\text{C13})$$

Appendix D: RG analysis

For completeness, in this appendix we provide the derivation of the flow equations for the Kondo couplings in the model (13) using the perturbative RG approach. (See, e.g., [41]). The (euclidean) action for the Kondo problem

corresponding to the Hamiltonian (13) is $S = S_0 + S_K$, where

$$S_0 = \sum_{j=1,2} \int \frac{d\omega}{2\pi} |\omega| |\varphi_j(\omega)|^2, \quad (D1)$$

$$S_K = \sum_{j=1,2} \int dt \left[\frac{-i\tilde{J}'_{z,j}}{\sqrt{\pi}u_j} \partial_t \varphi_j \sigma^z + \frac{J_{\perp,j}}{2\pi\xi_j} \left(e^{i2\sqrt{\pi}\kappa_j\varphi_j} \sigma^+ + e^{-i2\sqrt{\pi}\kappa_j\varphi_j} \sigma^- \right) \right]. \quad (D2)$$

Here we use the notation $\varphi_j(t) \equiv \tilde{\phi}_j(0, t)$, and t denotes imaginary time. Following [41] S_0 is obtained by integrating out $\varphi_j(x \neq 0, t)$. The action S contains a large frequency cutoff Λ , i.e., $|\omega| < \Lambda$ in all frequency integrations, where we identify $\Lambda = \frac{u_j}{\xi_j}$.

The RG approach proceeds as follows [41, 42]. We introduce a rescaled cutoff $\Lambda' = \Lambda/b$, where $b = e^\ell > 1$ is a scaling factor, with $\ell \ll 1$. We separate the field into slow and fast components, $\varphi_j = \varphi_j^< + \varphi_j^>$, where the first contains only frequency components smaller than Λ' , and the latter contains frequency components between Λ' and Λ . We further note $\vec{\sigma} = \vec{\sigma}_< + \vec{\sigma}_>$. We are using time-ordered bosonic correlation, hence for consistency of the calculation one has to use the time-ordered product of impurity spins as well. This is given by $\mathcal{T}[\sigma_z^\pm(\tau)\sigma_z^\mp(\tau')] = \frac{1}{2} + \sigma_z^\pm \text{sgn}(\tau - \tau')$ [41]. We then integrate over the fast component, and obtain an effective action for the slow component, which has the same form as the original action, but with renormalized coefficients, from which we can read the RG equations.

After integrating out the fast modes, the effective action for the slow modes up to second order in the Kondo couplings takes the following expression:

$$S_{\text{eff}}[\varphi^<] = S_0[\varphi^<] + \langle S_K[\varphi] \rangle_> - \frac{1}{2} (\langle S_K^2[\varphi] \rangle_> - \langle S_K[\varphi] \rangle_>^2), \quad (D3)$$

where $\langle \dots \rangle_>$ denotes the integration over the fast modes, i.e., using the action $S_0[\varphi^>]$. Let us begin with the calculation of the first order correction. Here, we have used $\langle \partial_t \varphi_j \rangle_> = \partial_t \varphi_j^<$ and $\langle (\varphi_j^>)^2 \rangle_> = \frac{1}{2\pi} \log b$. We now need to restore the cutoff to its original value Λ , which can be accomplished by rescaling the time $t \rightarrow bt$ and redefining the field $\varphi_j^<(t) \rightarrow \varphi_j^<(bt) \equiv \bar{\varphi}(t)$. Then we get

$$\langle S_K[\varphi] \rangle_> = \sum_j \int dt \left[\frac{-i\tilde{J}'_{z,j}}{\sqrt{\pi}u_j} \partial_t \bar{\varphi}_j \sigma^z + \frac{J_{\perp,j} b^{1-\kappa_j^2}}{2\pi\xi_j} \left(e^{i2\sqrt{\pi}\kappa_j\bar{\varphi}_j} \sigma^+ + e^{-i2\sqrt{\pi}\kappa_j\bar{\varphi}_j} \sigma^- \right) \right]. \quad (D4)$$

This results implies that $\tilde{J}'_{z,j}$ is not renormalized at first order, while for $J_{\perp,j}$ we find

$$\frac{dJ_{\perp,j}}{d\ell} = (1 - \kappa_j^2) J_{\perp,j}.$$

At second order we find

$$\begin{aligned} \langle S_K^2[\varphi] \rangle_> &= \sum_{j_1, j_2} \int dt_1 dt_2 \left\langle \left[\frac{-i\tilde{J}'_{z,j_1}}{\sqrt{\pi}u_{j_1}} \partial_t \varphi_{j_1}(t_1) \sigma^z + \frac{J_{\perp,j_1}}{2\pi\xi_{j_1}} \left(e^{i2\sqrt{\pi}\kappa_{j_1}\varphi_{j_1}(t_1)} \sigma^+ + e^{-i2\sqrt{\pi}\kappa_{j_1}\varphi_{j_1}(t_1)} \sigma^- \right) \right] \times \right. \\ &\times \left. \left[\frac{-i\tilde{J}'_{z,j_2}}{\sqrt{\pi}u_{j_2}} \partial_t \varphi_{j_2}(t_2) \sigma^z + \frac{J_{\perp,j_2}}{2\pi\xi_{j_2}} \left(e^{i2\sqrt{\pi}\kappa_{j_2}\varphi_{j_2}(t_2)} \sigma^+ + e^{-i2\sqrt{\pi}\kappa_{j_2}\varphi_{j_2}(t_2)} \sigma^- \right) \right] \right\rangle_>. \end{aligned} \quad (D5)$$

We calculate only the quantity of interest:

$$\left\langle e^{i2s\sqrt{\pi}\kappa_j\varphi_j(\tau)} \partial_{\tau'} \varphi_j^>(\tau') \right\rangle_> = -\frac{2s\sqrt{\pi}}{ib\kappa_j} e^{i2s\sqrt{\pi}\kappa_j\varphi_j^<(\tau)} \kappa_j \partial_{\tau'} \langle \varphi_j^>(\tau) \varphi_j^>(\tau') \rangle_>. \quad (D6)$$

Next, we perform the change of variables $t = \tau - \tau'$ and $T = \frac{\tau + \tau'}{2}$. We rescale the variable $b\bar{\tau} = \tau$ as well as the fields $\bar{\varphi}_j(\bar{\tau})$. Hence one can finally write

$$\begin{aligned} \langle S_K \rangle_> &= \int d\bar{\tau} \left[\frac{-i\tilde{J}'_{z,j}}{\sqrt{\pi}u_j} \partial_{\bar{\tau}} \bar{\varphi}_j(\bar{\tau}) \sigma^z + \frac{J_{\perp,j}}{2\pi\xi} \left(1 + (\kappa_j^2 - 1) \frac{\delta\Lambda}{\Lambda} \right) \left(e^{i2\sqrt{\pi}\kappa_j\bar{\varphi}_j(\bar{\tau})} \sigma^+ + e^{-i2\sqrt{\pi}\kappa_j\bar{\varphi}_j(\bar{\tau})} \sigma^- \right) \right], \\ -\frac{1}{2} (\langle S_K^2 \rangle_> - \langle S_K \rangle_>^2) &= \sum_{j=1}^2 \kappa_j \int dT \frac{J_{\perp,j} \tilde{J}'_{z,j}}{2\pi^2 \xi_j u_j} \ln(b) \left[e^{i2\sqrt{\pi}\kappa_j\varphi_j^<(T)} \sigma^+ + e^{-i2\sqrt{\pi}\kappa_j\varphi_j^<(T)} \sigma^- \right] \\ &\quad - \sum_{j=1}^2 \frac{(J_{\perp,j})^2}{(2\pi)^2 \xi_j^2} 4\sqrt{\pi}\kappa_j^3 i\sigma^z \int dT \partial_T \varphi_j^<(T) \frac{1}{\Lambda^2} d\ell. \end{aligned} \quad (D7)$$

We then arrive at the effective action with rescaled couplings

$$S_{\text{eff}}[\bar{\varphi}] = S_0[\bar{\varphi}] + \int dt \left[\frac{-i\tilde{J}'_{z,j}(l)}{\sqrt{\pi}u_j} \partial_t \bar{\varphi}_j(t) \sigma^z + \frac{J_{\perp,j}(l)}{2\pi\xi_j} \left(e^{i2\sqrt{\pi}\kappa_j\bar{\varphi}_j(t)} \sigma^+ + e^{-i2\sqrt{\pi}\kappa_j\bar{\varphi}_j(t)} \sigma^- \right) \right]. \quad (\text{D8})$$

where the couplings satisfy the following RG equations:

$$\frac{d\tilde{J}'_{z,j}}{dl} = \frac{\kappa_j^3}{\pi u_j} (J_{\perp,j})^2, \quad (\text{D9})$$

$$\frac{dJ_{\perp,j}}{dl} = (1 - \kappa_j^2) J_{\perp,j} + \frac{\kappa_j}{\pi u_j} \tilde{J}'_{z,j} J_{\perp,j}. \quad (\text{D10})$$

In terms of the unshifted couplings $\tilde{J}_{z,j}$, we find

$$\frac{d\tilde{J}_{z,j}}{dl} = \frac{\kappa_j^3}{\pi u_j} (J_{\perp,j})^2, \quad (\text{D11})$$

$$\begin{aligned} \frac{dJ_{\perp,j}}{dl} &= (1 - \kappa_j^2 - 2\kappa_j V_{\phi}^{\bar{j}j}) J_{\perp,j} + \frac{\kappa_j}{\pi u_j} \tilde{J}_{z,j} J_{\perp,j}, \\ &= (1 - (V_{\phi}^{jj})^2 - (V_{\phi}^{\bar{j}j})^2) J_{\perp,j} + \frac{\kappa_j}{\pi u_j} \tilde{J}_{z,j} J_{\perp,j}. \end{aligned} \quad (\text{D12})$$

The first term in the last line can be easily understood: it is the scaling dimension of the J_{\perp} operator in Eq. (11), after the diagonalization of the bulk Hamiltonian, but before any unitary transformation. In the limit of decoupled channels,

$$V_{\phi}^{ij} = \sqrt{K_j} \delta_{ij}, \quad V_{\theta}^{ij} = \delta_{ij} / \sqrt{K_j}, \quad \tilde{J}'_{z,j} = J_{z,j} / \sqrt{K_j}, \quad \kappa_j = \sqrt{K_j},$$

and we find

$$\frac{dJ_{z,j}}{dl} = \frac{K_j^2}{\pi u_j} (J_{\perp,j})^2, \quad (\text{D13})$$

$$\frac{dJ_{\perp,j}}{dl} = (1 - K_j) J_{\perp,j} + \frac{1}{\pi u_j} J_{z,j} J_{\perp,j}, \quad (\text{D14})$$

which differs from the RG equations of [41]. The equations differ from those in [18], which read

$$\frac{dJ_{z,j}}{dl} = \frac{1}{\pi u_j} (J_{\perp,j})^2, \quad (\text{D15})$$

$$\frac{dJ_{\perp,j}}{dl} = (1 - K_j) J_{\perp,j} + \frac{1}{\pi u_j} J_{z,j} J_{\perp,j}. \quad (\text{D16})$$

This can be understood as due to the fact that the equations in [18] are meant to be valid for weak e-e interactions, i.e., $K_j \approx 1$ (see comment in [41]).

We notice that the equation for $J_{\perp,j}$ can be easily obtained by using the Hamiltonian (15). Indeed, in this case we just need the scaling dimension of the J_{\perp} operator:

$$\frac{dJ_{\perp,j}}{dl} = (1 - \sum_k \kappa_{jk}^2) J_{\perp,j}. \quad (\text{D17})$$

We observe that

$$\sum_k \kappa_{jk}^2 = \sum_k \left(V_{\phi}^{jk} - \frac{\tilde{J}_{z,k}}{2\pi u_k} \right)^2 = \sum_k \left(V_{\phi}^{jk} - \frac{\tilde{J}'_{z,k}}{2\pi u_k} - V_{\phi}^{\bar{k}k} \right)^2, \quad (\text{D18})$$

$$\approx \left(V_{\phi}^{jj} - V_{\phi}^{\bar{j}j} \right)^2 - \left(V_{\phi}^{jj} - V_{\phi}^{\bar{j}j} \right)^2 \frac{\tilde{J}'_{z,j}}{\pi u_j} = \kappa_j^2 - \frac{\kappa_j}{\pi u_j} \tilde{J}'_{z,j}. \quad (\text{D19})$$

In the last line we used the definition of $\tilde{J}'_{z,j}$ in Eq. (14) and we omitted terms of order \tilde{J}'^2 . Inserting this expression in Eq. (D17) we recover Eq. (D10).

Appendix E: Conductance for weak coupling

In this section we give some details of the calculation of the correction to the conductance at finite temperature and frequency. We start with the Hamiltonian \tilde{H} in Eq. (15), which we rewrite here for convenience:

$$\tilde{H} = \sum_{j=1,2} \left[\frac{u_j}{2} \int dx \left[\tilde{\Pi}_j^2 + (\partial_x \tilde{\phi}_j)^2 \right] + \frac{J_{\perp,j}}{2\pi\xi_j} \left(e^{i2\sqrt{\pi} \sum_k \kappa_{jk} \tilde{\phi}_k(0)} \sigma^+ + \text{h.c.} \right) \right]. \quad (\text{E1})$$

The spin flip current is given by $\delta I = -e\partial_t \sigma^z$ [19]. In our case this expression turns out to be

$$\delta I = ie \sum_{j=1,2} \frac{J_{\perp,j}}{2\pi\xi_j} \left[e^{i2\sqrt{\pi} \sum_k \kappa_{jk} \tilde{\phi}_k} \sigma^+ - e^{-i2\sqrt{\pi} \sum_k \kappa_{jk} \tilde{\phi}_k} \sigma^- \right]. \quad (\text{E2})$$

The correction to the conductance $\delta\mathcal{G}(\omega)$ can be computed using the Kubo formula [21, 40], which amounts to calculating the current-current correlator from Eq. (E2) [19, 21]. For these calculations one needs to use the finite temperature bosonic correlators defined as [31, 32]

$$\langle \mathcal{T} \left[\tilde{\phi}_j(\tau) - \tilde{\phi}_j(0) \right]^2 \rangle = \frac{1}{2\pi} \log \left[\left(\frac{\beta u_j}{\pi \xi_j} \right)^2 \sin^2 \left(\frac{\pi}{\beta} \tau \right) \right], \quad (\text{E3})$$

where τ is imaginary time, $\beta = 1/T$, and $\xi_j = u_j/\Lambda$. We then obtain $\delta\mathcal{G}(\omega) = I_1 + I_2 + I_3$, where

$$\begin{aligned} I_1 &= -2e^2 \left(\frac{J_{\perp,1}}{2\pi\xi_1} \right)^2 \left(\frac{\pi\xi_1}{\beta u_1} \right)^{2\kappa_{11}^2} \left(\frac{\pi\xi_2}{\beta u_2} \right)^{2\kappa_{12}^2} \sin(\pi(\kappa_{11}^2 + \kappa_{12}^2)) \int_0^\infty dt \frac{(e^{i\omega t} - 1)/i\omega}{|\sinh(\frac{\pi}{\beta}t)|^{2(\kappa_{11}^2 + \kappa_{12}^2)}}, \\ I_2 &= -2e^2 \left(\frac{J_{\perp,2}}{2\pi\xi_2} \right)^2 \left(\frac{\pi\xi_1}{\beta u_1} \right)^{2\kappa_{21}^2} \left(\frac{\pi\xi_2}{\beta u_2} \right)^{2\kappa_{22}^2} \sin(\pi(\kappa_{21}^2 + \kappa_{22}^2)) \int_0^\infty dt \frac{(e^{i\omega t} - 1)/i\omega}{|\sinh(\frac{\pi}{\beta}t)|^{2(\kappa_{21}^2 + \kappa_{22}^2)}}, \\ I_3 &= -4e^2 \frac{J_{\perp,1}J_{\perp,2}}{(2\pi)^2\xi_1\xi_2} \left(\frac{\pi\xi_1}{\beta u_1} \right)^{2(\kappa_{11}\kappa_{12})} \left(\frac{\pi\xi_2}{\beta u_2} \right)^{2\kappa_{22}\kappa_{21}} \sin(\pi(\kappa_{11}\kappa_{12} + \kappa_{22}\kappa_{21})) \int_0^\infty dt \frac{(e^{i\omega t} - 1)/i\omega}{|\sinh(\frac{\pi}{\beta}t)|^{2(\kappa_{11}\kappa_{12} + \kappa_{22}\kappa_{21})}}. \end{aligned} \quad (\text{E4})$$

In the limit $J_{\perp,j}^2 \ll \omega \ll T$ we can simplify the above expressions as follows:

$$\begin{aligned} I_1 &= -\frac{e^2}{4} \left(\frac{J_{\perp,1}}{2\pi\xi_1} \right)^2 \left(\frac{2\pi T}{\Lambda} \right)^{2\kappa_{11}^2} \left(\frac{2\pi T}{\Lambda} \right)^{2\kappa_{12}^2} \left(\frac{1}{\pi T} \right)^2 \frac{\pi\Gamma(\kappa_{11}^2 + \kappa_{12}^2)^2}{\Gamma(2(\kappa_{11}^2 + \kappa_{12}^2))}, \\ I_2 &= -\frac{e^2}{4} \left(\frac{J_{\perp,2}}{2\pi\xi_2} \right)^2 \left(\frac{2\pi T}{\Lambda} \right)^{2\kappa_{21}^2} \left(\frac{2\pi T}{\Lambda} \right)^{2\kappa_{22}^2} \left(\frac{1}{\pi T} \right)^2 \frac{\pi\Gamma(\kappa_{21}^2 + \kappa_{22}^2)^2}{\Gamma(2(\kappa_{21}^2 + \kappa_{22}^2))}, \\ I_3 &= -\frac{e^2}{2} \frac{J_{\perp,1}J_{\perp,2}}{(2\pi)^2\xi_1\xi_2} \left(\frac{2\pi T}{\Lambda} \right)^{2(\kappa_{11}\kappa_{12})} \left(\frac{2\pi T}{\Lambda} \right)^{2\kappa_{22}\kappa_{21}} \left(\frac{1}{\pi T} \right)^2 \frac{\pi\Gamma(\kappa_{11}\kappa_{12} + \kappa_{22}\kappa_{21})^2}{\Gamma(2(\kappa_{11}\kappa_{12} + \kappa_{22}\kappa_{21}))}. \end{aligned} \quad (\text{E5})$$

From Eq. (E4) we see that I_3 vanishes in the exactly solvable limit. This shows that in this limit the correction takes the form of a sum of two contributions coming from two effectively independent channels, as in the case of the level width of the spectral function in Sec. III.

-
- [1] F. D. M. Haldane, Model for a Quantum Hall Effect without Landau Levels: Condensed-Matter Realization of the "Parity Anomaly", *Phys. Rev. Lett.* **61**, 2015 (1988).
 [2] B. A. Bernevig, Topological Insulators and Topological Superconductors, *Princeton: Princeton University Press* (2013).

- [3] M. Z. Hasan and C. L. Kane, Colloquium: Topological insulators, *Rev. Mod. Phys.* **82**, 3045 (2010).
 [4] C. L. Kane and E. J. Mele, Quantum spin hall effect in graphene, *Phys. Rev. Lett.* **95**, 226801 (2005).
 [5] C. L. Kane and E. J. Mele, \mathbb{Z}_2 topological order and the quantum spin hall effect, *Phys. Rev. Lett.* **95**, 146802 (2005).

- (2005).
- [6] B. A. Bernevig and S.-C. Zhang, Quantum Spin Hall Effect, *Phys. Rev. Lett.* **96**, 106802 (2006).
- [7] C. Wu, B. A. Bernevig, and S.-C. Zhang, Helical liquid and the edge of quantum spin hall systems, *Phys. Rev. Lett.* **96**, 106401 (2006).
- [8] C. Xu and J. E. Moore, Stability of the quantum spin hall effect: Effects of interactions, disorder, and Z₂ topology, *Phys. Rev. B* **73**, 045322 (2006).
- [9] Y. Tanaka and N. Nagaosa, Two interacting helical edge modes in quantum spin hall systems, *Phys. Rev. Lett.* **103**, 166403 (2009).
- [10] P. W. Anderson, A poor man's derivation of scaling laws for the kondo problem, *J. Phys. C* **3**, 2436 (1970).
- [11] P. Nozières and A. Blandin, Kondo effect in real metals, *J. Physique* **41**, 193 (1980).
- [12] M. Fabrizio, A. O. Gogolin, and P. Nozières, Anderson-Yuval approach to the multichannel kondo problem, *Phys. Rev. B* **51**, 16088 (1995).
- [13] P. Coleman and A. J. Schofield, Simple description of the anisotropic two-channel kondo problem, *Phys. Rev. Lett.* **75**, 2184 (1995).
- [14] D. L. Cox and A. Zawadowski, Exotic Kondo effects in metals: Magnetic ions in a crystalline electric field and tunnelling centres, *Adv. Phys.* **47**, 599 (1998).
- [15] A. C. Hewson, The Kondo Problem to Heavy Fermions, *Cambridge University Press, Cambridge, UK* (1993).
- [16] A. Furusaki and N. Nagaosa, Kondo Effect in a Tomonaga-Luttinger Liquid, *Phys. Rev. Lett.* **72**, 892 (1994).
- [17] A. Furusaki, Kondo Problems in Tomonaga-Luttinger Liquids, *J. Phys. Soc. Jpn.* **74**, 73 (2005).
- [18] J. Maciejko, C. Liu, Y. Oreg, X.-L. Qi, C. Wu, and S.-C. Zhang, Kondo effect in the helical edge liquid of the quantum spin hall state, *Phys. Rev. Lett.* **102**, 256803 (2009).
- [19] Y. Tanaka, A. Furusaki, and K. A. Matveev, Conductance of a helical edge liquid coupled to a magnetic impurity, *Phys. Rev. Lett.* **106**, 236402 (2011).
- [20] E. Eriksson, A. Ström, G. Sharma, and H. Johannesson, Electrical control of the kondo effect in a helical edge liquid, *Phys. Rev. B* **86**, 161103 (2012).
- [21] E. Eriksson, Spin-orbit interactions in a helical Luttinger liquid with a Kondo impurity, *Phys. Rev. B* **87**, 235414 (2013).
- [22] T. Posske, C.-X. Liu, J. C. Budich, and B. Trauzettel, Exact results for the Kondo screening cloud of two helical liquids, *Phys. Rev. Lett.* **110**, 016602 (2013).
- [23] T. Posske and B. Trauzettel, Direct proportionality between the Kondo cloud and current cross correlations in helical liquids, *Phys. Rev. B* **89**, 075108 (2014).
- [24] K. T. Law, C. Y. Seng, P. A. Lee, and T. K. Ng, Quantum dot in a two-dimensional topological insulator: The two-channel Kondo fixed point, *Phys. Rev. B* **81**, 041305 (2010).
- [25] Y.-L. Lee and Y.-W. Lee, Electrically tunable two-channel Kondo fixed points in helical liquids, *Phys. Rev. B* **88**, 035112 (2013).
- [26] V. J. Emery and S. Kivelson, Mapping of the two-channel Kondo problem to a resonant-level model, *Phys. Rev. B* **46**, 10812 (1992).
- [27] G. Toulouse, Expression exacte de l'énergie de l'état de base de l'hamiltonien de Kondo pour une valeur particulière de J_z , *C. R. Acad. Sci. Ser. B268*, 1200 (1969).
- [28] G. Zaránd and J. von Delft, Analytical calculation of the finite-size crossover spectrum of the anisotropic two-channel Kondo model, *Phys. Rev. B* **61**, 6918 (2000).
- [29] V. Kagalovsky, I. V. Lerner, and I. V. Yurkevich, Local impurity in a multichannel Luttinger liquid, *Phys. Rev. B* **95**, 205122 (2017).
- [30] M. Jones, I. V. Lerner, and I. V. Yurkevich, Berezinskii-Kosterlitz-Thouless transition in disordered multichannel Luttinger liquids, *Phys. Rev. B* **96**, 174210 (2017).
- [31] T. Giamarchi, Quantum Physics in One Dimension, *Clarendon Press (London, 2004)*.
- [32] E. Fradkin, Field Theories of Condensed Matter Physics, *Cambridge University Press, (Cambridge, 2013)*.
- [33] A. O. Gogolin, A.A. Nersisyan, A.M. Tsvelik, Bosonization and Strongly Correlated Systems, *Cambridge University Press (Cambridge, 1998)*.
- [34] I. V. Yurkevich, Duality in multichannel Luttinger liquid with local scatterer, *Europhys. Lett.* **104**, 37004 (2013).
- [35] I. V. Yurkevich and V. Kagalovsky, Superconducting edge states in a topological insulator, *Sci. Rep.* **11**, 18400 (2021).
- [36] R. A. Santos, D. B. Gutman, and S. T. Carr, Phase diagram of two interacting helical states, *Phys. Rev. B* **93**, 235436 (2016).
- [37] V. Kagalovsky, A. L. Chudnovskiy, and I. V. Yurkevich, Stability of a topological insulator: Interactions, disorder, and parity of Kramers doublets, *Phys. Rev. B* **97**, 241116 (2018).
- [38] A. M. Sengupta and A. Georges, Emery-Kivelson solution of the two-channel Kondo problem, *Phys. Rev. B* **49**, 10020 (1994).
- [39] I. Affleck, Conformal Field Theory Approach to the Kondo Effect, *Acta Phys. Polon. B* **26**, 1869 (1995).
- [40] P. Coleman, Introduction to Many-Body Physics, *Cambridge University Press* (2015).
- [41] J. Maciejko, Kondo lattice on the edge of a two-dimensional topological insulator, *Phys. Rev. B* **85**, 245108 (2012).
- [42] A. Altland and B. D. Simons, Condensed matter Field Theory, *Cambridge University Press* (2010).
- [43] R. Leturcq, L. Schmid, K. Ensslin, Y. Meir, D. C. Driscoll, and A. C. Gossard, Probing the Kondo Density of States in a Three-Terminal Quantum Ring, *Phys. Rev. Lett.* **95**, 126603 (2005).
- [44] J. Nygård, D. Cobden, and P. Lindelof, Kondo physics in carbon nanotubes, *Nature* **408**, 342 (2000).
- [45] J. Martinek, M. Sindel, L. Borda, J. Barnaś, J. König, G. Schön, and J. von Delft, Kondo Effect in the Presence of Itinerant-Electron Ferromagnetism Studied with the Numerical Renormalization Group Method, *Phys. Rev. Lett.* **91**, 247202 (2003).
- [46] L. Kouwenhoven and L. Glazman, Revival of the Kondo effect, *Phys. World* **14**, 33 (2001).